Role of vertex corrections in the matrix formulation of the random phase approximation for the multiorbital Hubbard model

Michaela Altmeyer, Daniel Guterding, P. J. Hirschfeld, Thomas A. Maier, Roser Valentí, and Douglas J. Scalapino

Phys. Rev. B **94**, 214515 — Published 21 December 2016

DOI: 10.1103/PhysRevB.94.214515

Role of vertex corrections in the matrix formulation of the random phase approximation for the multi-orbital Hubbard model

Michaela Altmeyer,[1] Daniel Guterding,[1] P. J. Hirschfeld,[2]
Thomas A. Maier,[3] Roser Valentí,[1] and Douglas J. Scalapino[4]

[1] *Institut für Theoretische Physik, Goethe-Universität Frankfurt, Max-von-Laue-Straße 1, 60438 Frankfurt am Main, Germany*
[2] *Department of Physics, University of Florida, Gainesville, FL 32611, USA*
[3] *Center for Nanophase Materials Sciences and Computer Science and Mathematics Division, Oak Ridge National Laboratory, Oak Ridge, TN 37831-6494, USA*
[4] *Department of Physics, University of California, Santa Barbara, CA 93106-9530, USA*

In the framework of a multi-orbital Hubbard model description of superconductivity, a matrix formulation of the superconducting pairing interaction that has been widely used is designed to treat spin, charge and orbital fluctuations within a random phase approximation (RPA). In terms of Feynman diagrams, this takes into account particle-hole ladder and bubble contributions as expected. It turns out, however, that this matrix formulation also generates additional terms which have the diagrammatic structure of vertex corrections. Here we examine these terms and discuss the relationship between the matrix-RPA superconducting pairing interaction and the Feynman diagrams that it sums.

I. INTRODUCTION

Despite considerable experimental and theoretical efforts over the last decades, unconventional superconductivity remains one of the most interesting open puzzles in solid state physics. While it has been proposed that in some unconventional superconductors several interactions may be responsible for superconductivity, spin fluctuations are argued by a large fraction of the solid state community to be the dominant mechanism driving Cooper pairing in heavy-fermion systems, cuprates, two-dimensional organic charge transfer salts and the iron based superconductors[1–4]. Such a statement is based on a few properties that have been found to be characteristic for these material classes like the fact that the superconducting phase is located in close vicinity to an antiferromagnetic ordered state and the phase transition can be easily tuned by application of pressure or charge doping[3,5–8].

Assuming spin, charge, and orbital fluctuations provide the dominant mechanism driving superconductivity, various theoretical approaches have been developed in the last decades in order to predict superconducting gap functions, critical temperatures and functional characteristics of thermodynamic quantities. Here we shall focus on the random phase approximation (RPA) for the Hubbard model. In the single-orbital case on a three-dimensional cubic lattice this approach leads to a strong enhancement of the singlet coupling in the proximity of a spin-density wave instability yielding to a $d_{x^2-y^2}$ symmetry of the gap function[9] as observed, for instance, in the high-T_c cuprates[10]. Also for superconducting organic charge transfer salts[11,12] this approximation seems to correctly predict the symmetry of the superconducting gap[13,14]. Recently, such an approximation has been successfully used for the determination of the superconducting gap structure in iron based superconductors and heavy fermion systems[15–22].

While the properties of high-Tc cuprates or organic charge transfer salts are well captured by single-orbital models,[23,24] it is crucial to consider multi-orbital models[15,25–29] when aiming for a proper description of heavy fermion systems and iron based superconductors[30,31]. Here the Fermi surfaces consist of several sheets, which emerge from various orbitals at the Fermi level that participate in the interactions driving superconductivity.

The matrix-RPA formulation for the single- and multi-orbital Hubbard model, as other RPA approaches, is built around the idea that terms involving particle-hole susceptibilities associated with a given wave-vector q and frequency ω add up coherently, while other terms have a *'random phase'* which suppresses their contribution. Neglection of these *'random phase'* terms in the calculation of the two-particle pairing vertex in the single-orbital case results in a summation of infinite orders of diagrams of pure bubble and ladder topology, yielding an easy-to-evaluate scalar closed-form expression for the pairing interaction. In the multi-orbital case, the susceptibilities acquire a complex orbital dependence and the interaction strength has to be replaced by full interaction matrices operating on the different orbitals.

In this work we examine the relation between (i) the diagrammatic representation of the random phase approximation to the two-particle vertex function in the context of the multi-orbital Hubbard model considering inter- and intra-orbital couplings and (ii) the corresponding matrix representation of the fluctuation exchange approximation[15,27,29]. The latter has been very commonly used to analyze superconductivity in multi-band systems, with the assumption that it was equivalent to the usual bubble and ladder diagams that occur in the one-band RPA.

In contrast to the derivation based on the separation

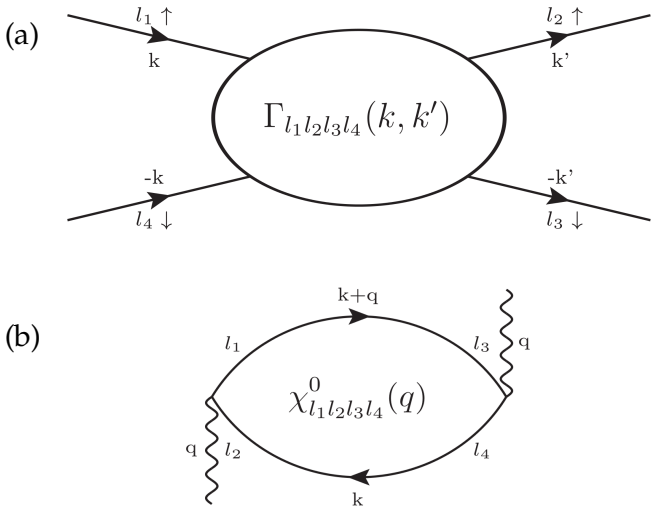

Figure 1. Diagrammatic structure of the (a) interaction vertex between two particles with opposite spin and momentum and the (b) matrix elements of the bare susceptibility.

into the different fluctuation channels[32], we follow the original diagrammatic approach[9] and write down all low order contributions to the two-particle vertex that can be rewritten as products of the interactions and the bare particle-hole susceptibilities. Applying this prescription to the single-orbital case, we recover the well-known result for the interaction vertex where only diagrams of pure bubble or ladder topology are incorporated. In contrast, in the multi-orbital case we find that, in addition to the diagrams that have the same topology as in the single-orbital case, there are additional diagrams that have the structure of vertex corrections. We analyze the contributions of such diagrams to certain elements of the pairing interaction and discuss their physical importance for the superconducting state.

II. THE MODEL

Understanding the relationship between the usual diagrammatic perturbation-resummation approach and the RPA matrix formulation provides insight into the physical processes that are captured in the latter. We are interested in relating the matrix-RPA form of the pairing vertex illustrated in Fig. 1(a) to its diagrammatic representation.

To illustrate our basic point, it is sufficient to consider a two-orbital problem, where the noninteracting part of the Hamiltonian, H_0, is diagonal in spin σ, but allows for hopping between the two orbitals ($l = 1$ or 2). Our discussion can easily be generalized to more than two orbitals. The noninteracting Hamiltonian is given by

$$H_0 = \sum_{\sigma l l' k} \left(\xi_{ll'}(k) + \epsilon_l \delta_{ll'}\right) d^\dagger_{l\sigma}(k) d_{l'\sigma}(k). \tag{1}$$

For the interacting part of our model Hamiltonian, $H_{\rm int}$, we first restrict ourselves to the intra- and inter-orbital Coulomb interactions U and U', as the effects we wish to discuss are included:

$$\begin{aligned} H_{\rm int} =& U \sum_{k,k',q,l} c^\dagger_{l\uparrow}(k+q) c^\dagger_{l\downarrow}(k'-q) c_{l\downarrow}(k') c_{l\uparrow}(k) \\ &+ \frac{U'}{2} \sum_{\substack{k,k',q,\\ l,l'\neq l,\sigma,\sigma'}} c^\dagger_{l\sigma}(k+q) c^\dagger_{l'\sigma'}(k'-q) c_{l'\sigma'}(k') c_{l\sigma}(k). \end{aligned} \tag{2}$$

We will discuss later what happens when Hund's rule exchange J and pair hopping J' are included.

For this model, the matrix-RPA pairing interaction in the singlet channel derived in the FLEX approximation[15,27–29] in the vicinity of the critical temperature, where the anomalous Green's function vanishes, has the following form:

$$\begin{aligned} \Gamma^{\rm RPA}_{l_1l_2l_3l_4}(k,k') = \Big[&\frac{3}{2} U^S \chi_1^{\rm RPA}(k-k') U^S \\ &- \frac{1}{2} U^C \chi_0^{\rm RPA}(k-k') U^C \\ &+ \frac{1}{2}\left(U^S + U^C\right) \Big]_{l_1l_2l_3l_4}. \end{aligned} \tag{3}$$

The spin and charge (also commonly called *orbital*) interaction matrices U^S and U^C respectively, are 4×4 matrices with indices $(l_1l_2) = (11, 22, 12, 21)$. Their explicit form is given by:

$$U^S = \begin{pmatrix} U & 0 & 0 & 0 \\ 0 & U & 0 & 0 \\ 0 & 0 & U' & 0 \\ 0 & 0 & 0 & U' \end{pmatrix} \tag{4a}$$

$$U^C = \begin{pmatrix} U & 2U' & 0 & 0 \\ 2U' & U & 0 & 0 \\ 0 & 0 & -U' & 0 \\ 0 & 0 & 0 & -U' \end{pmatrix} \tag{4b}$$

The RPA spin ($\chi_1^{\rm RPA}$) and charge ($\chi_0^{\rm RPA}$) susceptibilities for total spin zero have the form:

$$\chi_1^{\rm RPA}(q) = \left[1 - U^S \chi^0(q)\right]^{-1} \chi^0(q) \tag{5a}$$

$$\chi_0^{\rm RPA}(q) = \left[1 + U^C \chi^0(q)\right]^{-1} \chi^0(q) \tag{5b}$$

where the matrix elements of the bare susceptibility $\chi^0(q)$ are given by[15] (see Fig. 1(b)):

$$\begin{aligned} &\chi^0_{l_1l_2l_3l_4}(q,\omega_m) \\ &\quad = -\frac{T}{N} \sum_{k,\omega_n} G^0_{l_3l_1}(k+q, \omega_n+\omega_m) G^0_{l_2l_4}(k,\omega_n) \end{aligned} \tag{6}$$

Here, $G^0_{ll'}(k,\omega_n)$ denotes the bare Green's function

$$G^0_{ll'}(k,\omega_n) = \sum_\mu \frac{a^l_\mu(k) a^{l'*}_\mu(k)}{i\omega_n - \xi_\mu(k)} \tag{7}$$

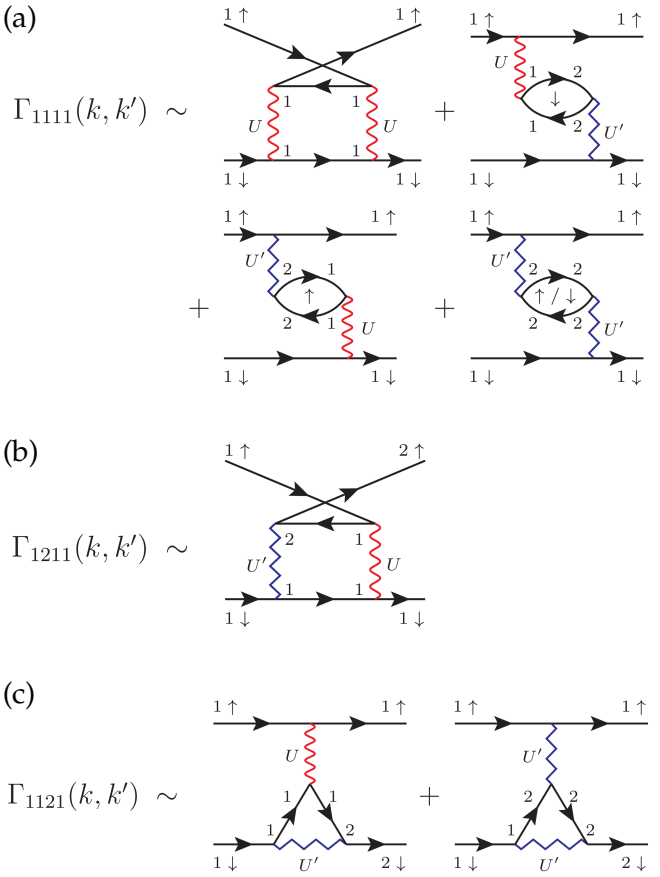

Figure 2. Feynman diagrams contributing to (a) $\Gamma_{1111}(k,k')$, (b) $\Gamma_{1211}(k,k')$, and (c) $\Gamma_{1121}(k,k')$.

for an electron with momentum k and Matsubara energy $\omega_n = (2n+1)\pi/\beta$ propagating between the l and l'-orbitals. The weights $a^l_\mu(k)$ are the l elements of the eigenvectors with eigenvalue $\xi_\mu(k)$, which are determined by diagonalization of the noninteracting tight-binding Hamiltonian (Eq. 1).

III. RESULTS

We begin our study of the relationship between the matrix formulation of the RPA pairing interaction $\Gamma^{\rm RPA}_{l_1l_2l_3l_4}(k,k')$ (Eq. 3) and the usual diagrammatic perturbation theory for $\Gamma_{l_1l_2l_3l_4}(k,k')$, by examining two second order contributions to $\Gamma^{\rm RPA}_{l_1l_2l_3l_4}(k,k')$, namely the index combinations $\{l_1l_2l_3l_4\} = \{1111\}$:

$$\Gamma^{\rm RPA}_{1111}(k,k') \sim U^2\chi^0_{1111}(k-k') - UU'\chi^0_{1122}(k-k') - UU'\chi^0_{2211}(k-k') - 2U'^2\chi^0_{2222}(k-k') \quad (8)$$

and $\{1121\}$:

$$\Gamma^{\rm RPA}_{1121}(k,k') \sim 2UU'\chi^0_{1121}(k-k') + U'^2\chi^0_{2221}(k-k') \quad (9)$$

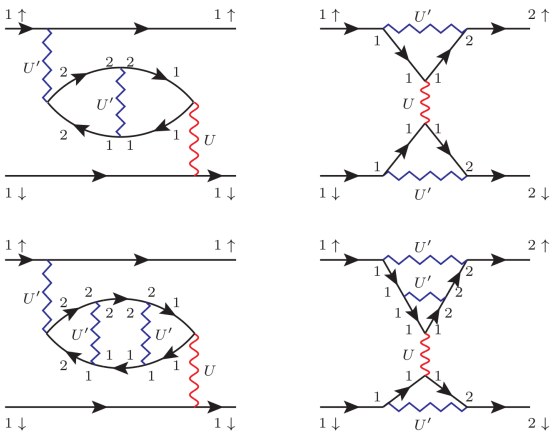

Figure 3. Examples of some 3rd and 4th order diagrams with U' vertex corrections which contribute to Γ_{1111} and Γ_{1221}.

Using the standard diagrammatic rules for $\Gamma_{1111}(k,k')$, the last three diagrams shown in Fig. 2(a) correspond to the last three terms in Eq. 8 for $\Gamma^{\rm RPA}_{1111}(k,k')$. The first diagram in Fig. 2(a) gives $U^2\chi^0_{1111}(k+k')$. For a singlet and even frequency particle pair the Pauli principle implies a certain symmetry of the vertex function:

$$\Gamma_{l_1l_2l_3l_4}(k,k') = \Gamma_{l_1l_3l_2l_4}(k,-k'). \quad (10)$$

As a consequence, $\Gamma_{1111}(k,k')$ is invariant under $k' \to -k'$ and the contribution from the first diagram in Fig. 2(a) corresponds indeed to the first contribution to the RPA expression in Eq. 8.

We investigate now the contributions to $\Gamma^{\rm RPA}_{1121}(k,k')$ (Eq. 9) and $\Gamma^{\rm RPA}_{1211}(k,k')$, which are related by symmetry in the singlet channel such that $\Gamma_{1211}(k,k') = \Gamma_{1121}(k,-k')$ (see Eq. 10). In the diagrammatic expansion of $\Gamma_{1211}(k,k')$ we have in second order a term of the form:

$$UU'\chi^0_{1121}(k+k') \quad (11)$$

as shown in Fig. 2(b). By symmetry this diagram corresponds to the first term in Eq. 9:

$$\Gamma^{\rm RPA}_{1121}(k,k') \sim UU'\chi^0_{1121}(k-k') \quad (12)$$

The remaining contributions to $\Gamma^{\rm RPA}_{1121}(k,k')$ (Eq. 9) are proportional to $UU'\chi^0_{1121}(k-k')$ and $U'^2\chi^0_{2221}(k-k')$ respectively. As the interorbital Coulomb repulsion preserves spin and orbital indices at each primitive vertex, a scheme only based on bubble and ladder diagrams leads to no contributions to $\Gamma^{\rm RPA}_{1121}(k,k')$. However, both terms in Eq. 9 can be rewritten as shown in Fig. 2(c) (left and right diagrams) and have the meaning of vertex corrections in the standard diagrammatic expansion. We note that the same type of vertex correction diagrams appear in functional renormalization group calculations for the multi-orbital Hubbard model[33].

For higher orders, the Feynman diagrams that contribute to $\Gamma^{\rm RPA}_{l_1l_2l_3l_4}$ consist of the familiar bubble and

particle-hole ladder diagrams as well as diagrams that can be rewritten as vertex corrections arising from U'. Examples of higher order vertex contributions are illustrated in Fig. 3.

Note that there is a simple way to recognize the Feynman diagrams that are included in the matrix-RPA: If one can assign the internal propagators into pairs, such that the first propagator is created at the same interaction vertex at which the second propagator is annihilated and vice versa, then each pair corresponds to the bare susceptibility as given in Eq. (6) and the contribution of the considered Feynman diagram to the pairing interaction can be entirely written in terms of the interactions and the bare susceptibilities.

If a Hund's rule exchange J and a *'pair hopping'* term J' are included in the multi-orbital interaction (see e.g. Refs. 16 and 34) the interaction part of the Hamiltonian in real space is given by:

$$\begin{aligned} H_{\text{int}} =& U \sum_{i,l} n_{il\uparrow} n_{il\downarrow} + \frac{U'}{2} \sum_{i,l,l' \neq l} n_{il} n_{il'} \\ &+ \frac{J}{2} \sum_{\substack{i,l,l' \neq l \\ \sigma,\sigma'}} c^\dagger_{il\sigma} c^\dagger_{il'\sigma'} c_{il\sigma'} c_{il'\sigma} \\ &+ \frac{J'}{2} \sum_{i,l,l' \neq l,\sigma} c^\dagger_{il\sigma} c^\dagger_{il\bar{\sigma}} c_{il'\bar{\sigma}} c_{il'\sigma} \end{aligned} \tag{13}$$

and additional vertex terms appear in the diagrammatic expansion of the pairing interaction.

We analyze the contributions to the inter-orbital pair scattering process following Ref. 16: We only retain the diagonal terms of the bare susceptibilities $\chi_{abab}(q)$ with $a, b = 1, 2$, assuming that other terms are suppressed by matrix element effects (see also Eq. 7). We find that the dominant second order contribution ($J \ll U'$) to the pair scattering term Γ_{abba} originates in equal parts from ladder and vertex diagrams[35]. Summing higher order terms as shown in Fig. 4 we obtain the dominant term linear in J':

$$\Gamma^{\text{RPA}}_{1221}(k,k') \sim \frac{2J'U'\chi^0_{1212}(k-k')}{1-U'\chi^0_{1212}(k-k')} + \frac{2J'U'\chi^0_{2121}(k-k')}{1-U'\chi^0_{2121}(k-k')} \tag{14}$$

which contributes to $\Gamma^{\text{RPA}}_{1221}(k,k')$ (compare also to the results of the 3-orbital matrix-RPA as discussed in Ref. 16). For inversion symmetric systems the two contributions in Eq. 14 are equal, as the bare susceptibility (Eq. 6) obeys $\chi^0_{abcd}(q) = \chi^0_{dcba}(-q)$. A numerical analysis of the importance of these inter-orbital pair scattering terms Γ_{abba}, which we have shown to contain contributions arising from vertex correction diagrams, for a realistic model of the iron pnictides has recently been conducted by Kemper *et al.*[16]. Here, the authors find that in the presence of a nonvanishing pair hopping these terms critically influence the nodal structure of the superconducting gap (see also Fig. 9 of Ref. 16). Moreover, another recent study by Kontani *et al.*[36] has shown, that exactly the same terms may play a role in enhancing the electron-phonon coupling.

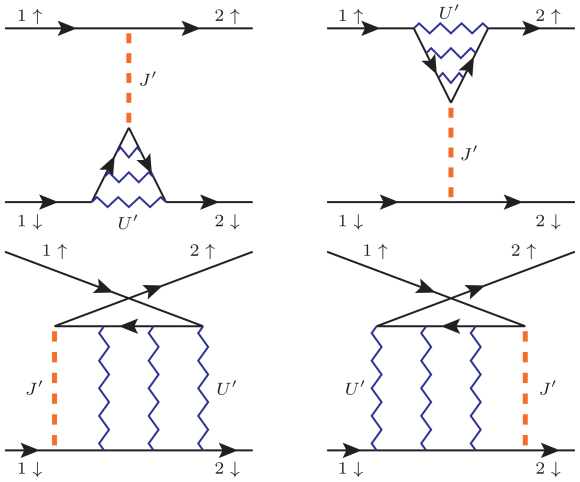

Figure 4. When the multiple scattering U' diagrams involving one factor of the pair hopping J' are summed they yield the leading J' result.

IV. CONCLUSIONS

Based on a simple two-orbital Hubbard model, we have analyzed the relationship between the matrix-RPA and the Feynman diagram technique for the calculation of the superconducting pairing interaction. In the single-orbital case, the diagrams corresponding to the matrix-RPA have been found to have a simple well-known structure containing only bubble or ladder subunits. In the multi-orbital case, the interorbital Coulomb interaction U' and an exchange pair hopping interaction J' generate additional diagrams that, as we have shown, have the structure of vertex corrections.

The matrix-RPA in the context of the multi-orbital Hubbard model is therefore a significant generalization of the commonly used random phase approximation: it is comprised of infinite order diagrams that can be written as products of the interactions and the bare susceptibilities. These include both the usual particle-hole bubble or ladder contributions, as well as the vertex corrections discussed here, all of which may be summed to infinite order in the usual RPA manner. We have therefore shown that the commonly used matrix-RPA expression for the pairing vertex in the multi-orbital Hubbard model provides a hitherto unappreciated method to keep additional contributions to infinite order beyond RPA. These additional diagrams are important in view of recent studies, as they significantly influence the node structure of the superconducting gap function[16], and may also enhance phonon-mediated interactions[36].

ACKNOWLEDGMENTS

We would like to thank K. Zantout, A. Rømer, Y. Wang, P. Lange, P. Kopietz and C. Gros for useful discussions. MA, DG and RV thank the German Research Foundation (Deutsche Forschungsgemeinschaft) for support through grants SFB/TR49 and SPP1458. PH acknowledges support through Department of Energy DE-FG02-05ER46236. TAM and DJS acknowledge support through the Center for Nanophase Materials Science at ORNL, which is sponsored by the Division of Scientific User Facilities, U.S. DOE. MA and RV further acknowledge partial support by the Kavli Institute for Theoretical Physics at the University of California, Santa Barbara under NSF Grant No. PHY11-25915.

[1] D. J. Scalapino, *A common thread: The pairing interaction for unconventional superconductors*, Rev. Mod. Phys. **84**, 1383 (2012).

[2] A. Ardavan, S. Brown, S. Kagoshima, K. Kanoda, K. Kuroki, H. Mori, M. Ogata, S. Uji, and J. Wosnitza, *Recent Topics of Organic Superconductors*, J. Phys. Soc. Jpn. **81**, 011004 (2012).

[3] H. Hosono and K. Kuroki, *Iron-based superconductors: Current status of materials and pairing mechanism*, Physica C **514**, 399 (2015).

[4] P.J. Hirschfeld, *Using Gap Symmetry and Structure to Reveal the Pairing Mechanism in Fe-based Superconductors*, Comptes Rendus Physique **17**, 197 (2016).

[5] R. H. McKenzie, *Similarities Between Organic and Cuprate Superconductors*, Science **278**, 5339 (1997).

[6] N. Toyota, M. Lang, and J. Müller, *Low-Dimensional Molecular Metals*, Springer-Verlag Berlin Heidelberg (2007).

[7] C. C. Tsuei and J. R. Kirtley, *Pairing symmetry in cuprate superconductors*, Rev. Mod. Phys. **72**, 969 (2000).

[8] O. Stockert, S. Kirchner, F. Steglich, and Q. Si, *Superconductivity in Ce- and U-based '122' Heavy-Fermion Compounds*, J. Phys. Soc. Jpn. **81**, 011001 (2012).

[9] D. J. Scalapino, E. Loh, and J. E. Hirsch, *d-wave pairing near a spin-density-wave instability*, Phys. Rev. B **34**, 8190(R) (1986).

[10] D. J. Van Harlingen, *Phase-sensitive tests of the symmetry of the pairing state in the high-temperature superconductors - Evidence for $d_{x^2-y^2}$ symmetry*, Rev. Mod. Phys. **67**, 515 (1995).

[11] B. J. Powell, and R. H. McKenzie, *Strong electronic correlations in superconducting organic charge transfer salts*, J. Phys.: Condens. Matter **18**, R827 (2006).

[12] G. Saito, and Y. Yoshida, *Organic superconductors*, Chem. Rec. **11**, 124 (2011).

[13] D. Guterding, S. Diehl, M. Altmeyer, T. Methfessel, U. Tutsch, H. Schubert, M. Lang, J. Müller, M. Huth, H. O. Jeschke, R. Valentí, M. Jourdan, H.-J. Elmers, *Evidence for eight node mixed-symmetry superconductivity in a correlated organic metal*, Phys. Rev. Lett. **116**, 237001 (2016).

[14] D. Guterding, M. Altmeyer, H.O. Jeschke, and R. Valentí, *Near-degeneracy of extended $s+d_{x^2-y^2}$ and d_{xy} order parameters in quasi-two-dimensional organic superconductors*, arXiv:1605:07017.

[15] T. Takimoto, T. Hotta, and K. Ueda, *Strong-coupling theory of superconductivity in a degenerate Hubbard model*, Phys. Rev. B **69**, 104504 (2004).

[16] A. F. Kemper, T. A. Maier, S. Graser, H.-P. Cheng, P. J. Hirschfeld, and D. J. Scalapino, *Sensitivity of the superconducting state and magnetic susceptibility to key aspects of electronic structure in ferropnictides*, New J. Phys. **12**, 073030 (2010).

[17] Y. Wang, A. Kreisel, V. B. Zabolotnyy, S. V. Borisenko, B. Büchner, T. A. Maier, P. J. Hirschfeld, and D. J. Scalapino, *Superconducting gap in LiFeAs from three-dimensional spin-fluctuation pairing calculations*, Phys. Rev. B **88**, 174516 (2013).

[18] A. Kreisel, Y. Wang, T. A. Maier, P. J. Hirschfeld, and D. J. Scalapino, *Spin-fluctuations and superconductivity in $K_xFe_{2-y}Se_2$*, Phys. Rev. B **88**, 094522 (2013).

[19] K. Suzuki, H. Usui, S, Iimura, Y. Sato, S. Matsuishi, H. Hosono, and K. Kuroki, *Model of the Electronic Structure of Electron-Doped Iron-Based Superconductors: Evidence for Enhanced Spin Fluctuations by Diagonal Electron Hopping*, Phys. Rev. Lett. **113**, 027002 (2014).

[20] D. Guterding, H. O. Jeschke, P. J. Hirschfeld, and R. Valentí, *Unified picture of the doping dependence of superconducting transition temperatures in alkali metal/ammonia intercalated FeSe*, Phys. Rev. B **91**, 041112(R) (2015).

[21] D. Guterding, S. Backes, H. O. Jeschke, and R. Valentí, *Origin of the superconducting state in the collapsed tetragonal phase of KFe_2As_2*, Phys. Rev. B **91**, 140503(R) (2015).

[22] H. Arai, H. Usui, K. Suzuki, Y. Fuseya, and K. Kuroki, *Theoretical study of correlation between spin fluctuations and T_c in isovalent-doped 1111 iron-based superconductors*, Phys. Rev. B **91**, 134511 (2015).

[23] L. F. Feiner, J. H. Jefferson, and R. Raimondi, *Effective single-band Hubbard model for the cuprates: Coulomb interactions and apical oxygen*, Physica B **206**, 672 (1995).

[24] R. H. McKenzie, *A strongly correlated electron model for the layered organic superconductors κ-(BEDT-TTF)$_2$X*, Comments Cond. Matt. Phys. **18**, 309 (1998).

[25] T. Takimoto, *Orbital fluctuation-induced triplet superconductivity: Mechanism of superconductivity in Sr_2RuO_4*, Phys. Rev. B **62**, R14641 (2000).

[26] T. Takimoto, T. Hotta, T. Maehira, and K. Ueda, *Spin-fluctuation-induced superconductivity controlled by orbital fluctuation*, J. Phys.: Condens. Matter **14**, L369 (2002).

[27] K. Kubo and T. Hotta, *Orbital-Controlled Superconductivity in f-Electron Systems*, J. Phys. Soc. Jpn. **75**, 083702 (2006).

[28] K. Kuroki, H. Usui, S. Onari, R. Arita, and H. Aoki, *Pnictogen height as a possible switch between high-T_c nodeless and low-T_c nodal pairings in the iron-based superconductors*, Phys. Rev. B **79**, 224511 (2009).

[29] S. Graser, T. A. Maier, P. J. Hirschfeld, and D. J. Scalapino, *Near-degeneracy of several pairing channels in multiorbital models for the Fe pnictides*, New J. Phys. **11**, 025016 (2009).

[30] T. Maehira, T. Hotta, K. Ueda, and A. Hasegawa, *Relativistic Band-Structure Calculations for $CeTIn_5$ (T = Ir and Co) and Analysis of the Energy Bands by Using Tight-*

Binding Method, J. Phys. Soc. Jpn. **72**, 854 (2003).

[31] O. K. Andersen and L. Boeri, *On the multi-orbital band structure and itinerant magnetism of iron-based superconductors*, Ann. Phys. (Berlin) **523**, 8 (2011).

[32] J. Zhang, *Theory of spin-fluctuation induced superconductivity in iron-based superconductors*, PhD thesis (2011).

[33] F. Wang, H. Zhai, Y. Ran, A. Vishwanath, and D.-H. Lee, *Functional Renormalization-Group Study of the Pairing Symmetry and Pairing Mechanism of the FeAs-Based High-Temperature Superconductor*, Phys. Rev. Lett. **102**, 047005 (2009).

[34] K. Kubo, *Pairing symmetry in a two-orbital Hubbard model on a square lattice*, Phys. Rev. B **75**, 224509 (2007).

[35] For a comparison of the magnitudes of several matrix elements $\Gamma_{l_1 l_2 l_3 l_4}(k, k')$ for realistic model parameters we refer the reader to the calculations for the iron pnictide compound LaFeAsO presented in Ref. 16.

[36] H. Kontani and S. Onari, *Orbital-Fluctuation-Mediated Superconductivity in Iron Pnictides: Analysis of the Five-Orbital-Hubbard-Holstein Model*, Phys. Rev. Lett. **104**, 157001 (2010).